Recovery of ammonium by powder synthetic zeolites from wastewater effluents: optimization of the regeneration step

Xialei You[a], César Valderrama[a,*], Xavier Querol[c] and José Luis Cortina[a,b]

[a] Department of Chemical Engineering. Universitat Politècnica de Catalunya-Barcelona-TECH (UPC), Spain

[b] Water Technology Center, CETaqua, Carretera d'Esplugues 75, Cornellá de Llobregat, 08940 Spain

[c] Institute of Environmental Assessment and Water Research IDAEA, Consejo Superior de Investigaciones Científicas (CSIC) Barcelona

[*]Correspondence should be addressed to: César Valderrama

Departament of Chemical Engineering, Universitat Politècnica de Catalunya-Barcelona Tech

Avda. Diagonal, 647 (08028) Barcelona, Spain

Tel.: 93 401 66 45

Email: cesar.alberto.valderrama@upc.edu

Abstract

Nitrogen recovery and valorisation is gaining interest due to the current need for nitrogen removal, so it is of the great interest that ammonium selective sorbents be evaluated. In this study, a zeolitic material synthesized from coal fly ash (Ze-Na) in sodium form as well as its modification to potassium form (Ze-K) were evaluated as sorbent materials for the recovery of ammonium from wastewater effluents. The sorption performance was assessed through three consecutive sorption-desorption cycles reporting opposite behaviour in terms of ammonium sorption capacity. Decreasing in the case of Ze-Na and to slightly increase for Ze-K due to alkaline activation of zeolite surface. The maximum sorption capacities obtained were 109±4 mg

NH_4/g and 33±1 mg NH_4/g for Ze-Na and Ze-K, respectively. It is important to point out that in the case of Ze-Na, the maximum sorbent capacity was obtained during the first sorption cycle whereas in the case of Ze-K was obtained during the last working cycle due to the alkaline regeneration.

Kinetic studies showed that after every regeneration step, the sorption kinetics turns faster as alkaline desorption increased the zeolite specific surface, thus increasing the size of porous and enhancing the diffusion through the particle. Results obtained indicate that sorption capacity decreased significantly after every working cycle using Ze-Na whereas Ze-K followed the opposite behaviour despite its initial lower sorption capacity.

Keywords: zeolite; ammonium; phosphate; sorption; regeneration; nutrients recovery

1. Introduction

Conventional urban wastewater treatment trains are based on the conventional activated sludge (CAS) process, which convert and transform a potential energy (and other) resources (e.g., organic and inorganic pollution loads) into biosolids while consuming large amounts of energy for the aeration stage. The new paradigm on urban sanitation systems is focused on the resource recovery (nutrients and energy) and inspires a search for technologies devoted to source separation and to make them available for reuse. The novel treatment schemes proposed to achieve this objective includes processes such as mainstream partial nitritation/anammox, nanofiltration/reverse osmosis and nitrogen recovery by stripping or sorption (Scherson and Criddle 2014; Verstraete and Vlaeminck 2011).

New ammonium recovery technologies are needed in order to face new problems as i) the implementation of High Rate Activated Sludges (HRAS) which improves the energy recovery from

anaerobic digestion by producing high ammonium treated effluents (Jimenez et al. 2015) or ii) the need to recover nitrogen accounting for its nutrient value.

Alternative ammonium recovery treatments as striping and sorption processes using synthetic polymeric sorbents or polymeric membrane based technologies have been studied reporting difficulties in the integration of membrane processes (X. Zhang et al. 2013) and fouling events related to the presence of total suspended solids and dissolved organic matter (Diamantis et al. 2014; Mezohegyi et al. 2012). Then, inorganic materials as sorbent or as support for biological filters could represent a suitable option to promote ammonium removal and recovery due to their physico-chemical properties (Y. Yang et al. 2017).

Zeolites are a promising materials to be used as low-cost sorbent for wastewater treatment applications (Tashauoei et al. 2010). They have been widely studied for nutrients removal and recovery from wastewater as they report high internal porosity which allows water retention, a uniform particle size distribution, high cation-exchange capacity for nutrients retaining, specially ammonium ions (Kulasekaran Ramesh et al. 2011; Sherry 2003a). By applying several methods, different families of zeolites have been synthesised from fly ash, however, few have been successfully converted into pure-phase zeolites.

Many applications of zeolites in agriculture are being investigated, especially as a carrier for slow release fertilizers (K. Ramesh et al. 2010) as they reported the availability for improving soil physicochemical and microbial capacity (Abdi et al. 2006) and enhance the use of nitrogen and phosphorus (Gruener et al. 2003; Hua et al. 2006; McGilloway et al. 2003). For this purpose, recovery of ammonium by zeolites can represent many advantages as loaded zeolites could be used as slow release fertilizer.

Despite many studies have been reported for ammonium removal by biological treatment (Bassin et al. 2012; Marcelino et al. 2011), using polymeric sorbents and biochar (Kim et al. 2012; Takaya

et al. 2016) or natural granular zeolites (Guaya et al. 2015; Wu et al. 2006; B.-H. Zhang et al. 2007), most of the implementation work has been addressed to determine the sorption capacity of zeolites (Gupta et al. 2015) and limited effort has been developed on the engineering aspects of the validation of the integration of synthetic zeolites in continuous sorption-regeneration processes to evaluate their regenerability and reusability capacity from the loaded sorbent. Regenerated zeolites could be reused effectively and concentrated ammonium solutions can be used for fertilizer production resulting in a significant economic improvement towards traditional treatments.

This study describes the sorption-desorption performance of two modified zeolites (in sodium and potassium form) synthetized from coal fly ash, for removal and recovery of ammonium from water samples. Ammonium is commonly accompanied by phosphate in anaerobic side streams; thus, the synthetic zeolite was converted to the potassium form to promote the simultaneous recovery of ammonium (by ion exchange) and phosphate (by formation of mixed potassium phosphates). The ammonium concentration levels evaluated covered the two types of ammonium streams expected in new configurations of wastewater treatment plants incorporating high rate activated sludge: i) effluents from the biosorption reaction with ammonium levels up to 100 mgNH_4/L and ii) side streams from the sludge anaerobic digestion with ammonium levels up to 1000 mgNH_4/L.

The equilibrium isotherm studies were carried out in ammonium single and binary (ammonium chloride/sodium phosphate) solutions. Ammonium uptake rate limiting step was evaluated by modelling kinetic experimental data by Homogeneous Particle Diffusion Model (HPDM) and Shell Progressive Model (SPD). Finally, the evolution of equilibrium and kinetic performance through several sorption desorption working cycles were studied through alkaline regeneration of loaded zeolites. Potential regeneration of both zeolites forms were evaluated by using NaOH or KOH solutions.

2. Material and methods

2.1. Raw materials

Sodium zeolite (Ze-Na) was synthesized from Narcea coal fly ash by an optimized conventional zeolite synthesis method using a 3M NaOH solution at 125 ºC and 8h of reaction as reported elsewhere (Moreno et al. 2001; Querol et al. 1996).

2.2. Preparation of Potassium modified zeolite

The Ze-Na modification procedure was adapted from the method reported by Wu et al. (2006). A pre-treatment step was carried out as follows: 30 g of Ze-Na was placed in a flask and mixed with 250 mL of 1 mol/L NaOH solution. The slurry continuous was stirred at room temperature for 24 h. The solid phase was separated by filtration and was mixed with 250 mL of 1 mol/L KCl solution and the slurry stirred continuously at room temperature for 2 h. The salt treatment step was repeated four times. The solid phase was separated by filtration and washed with deionized water for several times in order to wash out residual salts. Finally, the modified zeolite (Ze-K) was dried in an oven at 50 ºC for 72 h and stored in airtight containers for subsequent experiments.

2.3. Equilibrium sorption experiments: single and binary systems

Equilibrium sorption experiments were carried out by using standard methodology described in previous works (You et al. 2015, 2016). For ammonium single experiments, 25 mL of ammonium solution (5–5000 mg/L) were mixed mechanically with 0.1 g of zeolites until equilibrium was achieved (24 h).

For the study of binary systems, the procedure was repeated with solutions containing ammonium in the concentration range of 2-3000 mg/L and phosphate in the concentration range

of 6-900 mg/L. After phase separation, total ammonium and phosphate concentration was determined by ionic chromatography (Dionex ICS1000 CS-16 (Vertex, Molins de Rei, Spain)).

2.4. Kinetic studies

For kinetic studies, 1 g of zeolite was added into a precipitate glass flask containing 250 mL of ammonium solution with concentration of 10 mg/L. The system was agitated with magnetic stirrers in order to maintain the sorbent suspended in the solution. Samples of 6 mL were taken every minute the first 10 minutes, every 5 minutes until 30 minutes and finally, every 30 minutes until 3 hours and one more sample until equilibrium at 24 hours.

The kinetic models used to describe kinetic data are two approaches widely employed for fitting ion exchange data (Guaya et al. 2015), the Homogeneous Particle Diffusion Model (HPDM) and the Shell Progressive Model (SPM) or Shrinking Core Model (Ferrier et al. 2016; Valderrama et al. 2010) (Supplementary Material).

2.5. Alkaline regeneration of loaded zeolites

For the regeneration of zeolites, 10 mL of NaOH or KOH 1 mol/L were putted in contact with Na-Ze and K-Ze, respectively, to each polyethylene tube containing loaded zeolites as described in section 2.3. The samples were mixed with a mechanical shaker (Heidolph Reax 2) at room temperature during 4 hours at constant agitation. After the zeolite was settled in the bottom of the polyethylene tube, the supernatant solutions were extracted with a Pasteur pipette stored in plastic bottles to squirrel away in the refrigerator. In order to clean up the samples, ultrapure water was added in each tube and a mechanical shaker was used to mix the zeolite sample during 4 hours at room temperature. Finally, the regenerated zeolites were dried in an oven at 50ºC for 72 h before being reused.

2.6. Characterization of zeolites

Raw and loaded samples of Ze-Na and Ze-K zeolites were washed with ultrapure water and then dried in the oven at 60 ºC during 24h for physicochemical characterization.

Morphology of the samples as well as their chemical composition were analysed by using a JEOL 3400 Field Emission Scanning Electron Microscope coupled to an Energy Dispersive Spectroscopy system (FSEM-EDS). Reported samples composition is the average of three analyses in different points of the sample.

The mineralogical composition was also analysed by using a Bruker D8 A25 Advance X-Ray Diffractometter. The specific surface of samples was determined by the nitrogen gas sorption method with an automatic sorption analyser (Micrometrics).

3. Results and discussion

3.1. Characterization of virgin zeolites

The FSEM-EDS analyses reported C, O, Na, Mg, Al, Si, Ca, Fe and Ti as the main elements on the Ze-Na composition (Table 1). In Ze-K sample, the potassium content increased from 2.2% to 11.9% reporting a total substitution of sodium and part of calcium and magnesium ions present in Ze-Na.

Table 1. Chemical composition (wt %) of raw Ze-Na and salt modified zeolite Ze-K

	C	O	Na	Mg	Al	Si	K	Ca	Fe	Ti
Ze-Na	5.6	51.3	8.4	0.7	9.6	17.9	2.2	1.5	2.7	0.8
Ze-K	15.7	45.4	-	0.5	7.6	13.7	11.9	1.1	3.7	0.4

As can be observed in the previous table, Ze-Na is a high Silica Aluminium Ratio (SAR) zeolite. Thus, shows more affinity towards monovalent ions than divalent ions, which results in a partial substitution of calcium and magnesium ions by potassium ions during the modification process.

The substitution of sodium by potassium ions was performed without heating as zeolites with SAR between 1.5 and 1.8 (1.7±0.1 in the case of Ze-Na and Ze-K) show more affinity for potassium than sodium ions (Pauling 1960; Sherry 2003b).

SEM images (Figure 1) shown a surface with homogeneous crystal size distribution for both Ze-Na and Ze-K samples indicating that salt modification not reported significant morphology modifications. This fact could be explained as the ion exchange was carried out at room temperature by same valence cations which not represents any significant modification on the zeolite structure. (Li et al. 2000).

Figure 1.

In the X-Ray Diffraction patterns of Ze-Na and Ze-K (Figure 2) were identified mullite ($Al_6Si_2O_{13}$), quartz (SiO_2) and potassium and sodium aluminium silicates as predominant phases.

Figure 2.

Moreover, BET isotherms reported a specific surface of 6.30 m^2/g for Ze-Na and 16.95 m^2/g for Ze-K. This increase on specific surface is mainly due to the treatment with chlorides during the modification step, as was also observed by Lin et al. (2013).

3.2. Ammonium sorption capacity: single and binary solutions

Ammonium experimental sorption equilibrium and predicted data based on Langmuir and Freundlich isotherms are shown in Figure 3 for single and binary experiments. The isotherms parameters (q_m, K_L and K, n) were determined from the linearized forms of Eqs. 1 and 2, and are summarised in Table 2.

$$q = \frac{K_L q_m C_e}{1 + K_L C_e} \quad (1)$$

$$q = KC_e^{\frac{1}{n}} \quad (2)$$

where, q_m is the maximum loading of the sorbent (mg sorbate/g zeolite), K_L is the Langmuir sorption constant (L/mg), K is the Freundlich sorption constant $(mg/g)(mg/L)^{-1/n}$ and n is the Freundlich exponent.

Figure 3.

Table 2. Langmuir and Freundlich isotherm parameters for ammonium removal onto Ze-Na and Ze-K.

Model		Langmuir			Freundlich		
System		R^2	K_L	q_m	R^2	K	n
Ze-Na	Single	0.99	$2.15x10^{-3}$	109±4	0.92	1.65	1.85
	Binary	0.99	$2.17x10^{-2}$	17±1	0.69	1.20	2.57
Ze-K	Single	0.99	$1.14x10^{-2}$	21±2	0.88	0.63	1.86
	Binary	0.99	$1.10x10^{-2}$	29±1	0.91	0.96	2.02

The experimental equilibrium data were properly described by Langmuir isotherm with a maximum loading capacity of 109±4 mg NH_4/g for ammonium single sorption by Ze-Na. Sorption capacity decreased significantly in binary system (Ze-Na) mainly due to high amount of sodium ions present in aqueous solution provided by sodium phosphate salt.

On the other hand, Ze-K reported markedly lower sorption capacity than Ze-Na in ammonium single system as K ions have higher affinity towards zeolites than sodium ions (Huang et al. 2015; Sherry 2003b). Thus, the ion exchange by ammonium ions present in aqueous solution is less favored. Moreover, the difference reported between ammonium single and binary system is not significant as in the t-test performed, the p-value obtained in a significant test was higher than

202 0.05 (0.179), which indicates that sodium ions present in aqueous solution as well as phosphate
203 do not have effect on ammonium sorption onto Ze-K.

204 In addition, none of the both zeolites reported a significant phosphate sorption capacity as
205 monovalent counter ions are not able to react with phosphate ions by the formation of insoluble
206 phosphate minerals. Thus, in order to achieve the simultaneous uptake of ammonium and
207 phosphate ions from aqueous solution, it would require the mixture of zeolites in sodium or
208 potassium form with modified zeolites containing divalent or trivalent cations (Guaya et al. 2015;
209 He et al. 2016).

210 Analysis of the loaded zeolites reported a decrease of sodium and potassium content in Ze-Na
211 and Ze-K, respectively. Furthermore, although neither Ze-Na nor Ze-K were efficient for
212 phosphate uptake, EDS results showed phosphorus content on zeolites, mainly due to the
213 phosphate present in aqueous solution which was not totally washed from analyzed loaded
214 samples.

215 Moreover, the SEM images of loaded Ze-Na and Ze-K are shown in Figure 4. It can be noticed
216 that the inner structure of Ze-K reports nor significant variations as hydrated NH_4^+ and K^+ ions
217 have the same ion radii (331 pm) whereas Na^+ is considerably larger (358 pm) (Mazloomi and
218 Jalali 2016).

219 **Figure 4**

220 A comparison of ammonium removal efficiency with other natural and synthetic zeolites is listed in
221 the Table 3. In can be observed that despite the maximum ammonium sorption capacity of tested
222 zeolites (Ze-Na and Ze-K) in binary test solutions, the obtained values are higher than the most of
223 studies reported in the literature.

224 Table 3. Comparison of ammonium removal efficiency in different zeolites

	Type	Test solution	q_m [mg/g]	Reference
Ze-Na	Synthetic zeolite	NH_4^+	109	This study
	Synthetic zeolite	$NH_4^+ + PO_4^{3-}$	17	This study
Ze-K	Synthetic zeolite	NH_4^+	21	This study
	Synthetic zeolite	$NH_4+ + PO_4^{3-}$	29	This study
CV-Z	Synthetic zeolite	NH_4^+	13.7	(Otal et al. 2013)
LC-Z	Synthetic zeolite	NH_4^+	28.7	(M. Zhang, Zhang, Xu, Han, Niu, Zhang, et al. 2011)
HC-Z	Synthetic zeolite	NH_4^+	6.1	(M. Zhang, Zhang, Xu, Han, Niu, Zhang, et al. 2011)
Zeolite-FM	Synthetic zeolite	NH_4^+	50.2	(M. Zhang, Zhang, Xu, Han, Niu, Tian, et al. 2011)
NaA zeolite/chitosan	Synthetic zeolite + polymer	NH_4^+	48.5	(K. Yang et al. 2014)
NaOH-activated zeolite	Activated natural zeolite	$NH_4+ + PO_4^{3-}$	23.9	(He et al. 2016)
NLZ	Modified natural zeolite	$NH_4+ + PO_4^{3-}$	21.2	(He et al. 2016)
CMZ zeolite	Natural zeolite	NH_4^+	13.0	(Millar et al. 2016)
ZA zeolite	Natural zeolite	NH_4^+	8.6	(Millar et al. 2016)
NaCl activated zeolite	Natural zeolite	NH_4^+	5.9	(Alshameri et al. 2014)
NaOH activated zeolite	Natural zeolite	NH_4^+	4.6	(Alshameri et al. 2014)

225

226 **3.3 Kinetic studies**

227 In kinetic studies using Ze-Na less than 10 minutes were necessary to achieve up to 70% and
228 almost 90% of total uptake for single and binary systems, respectively. In the case of Ze-K, the
229 kinetics was very fast, with more than 80% of total uptake during the first minute of

experimentation, making that kinetic models were not able to fit and describe the experimental data.

Thus, only data obtained from kinetic experiments using Ze-Na was fitted to the Eqs. S2-S6 and the results of the linear regression analysis are summarized in Table S1. It can be observed that diffusion coefficients obtained for single system were 1.07 x 10^{-11} and 1.25 x 10^{-11} m^2/s by HPDM and SPM models, respectively, while in the binary system the reported values were 3.58 x 10^{-11} and 2.29 x 10^{-11} m^2/s. These values are in the same order of magnitude than those reported for Ag^+, Na^+ or Li^+ ions (M. Auerbach et al. 2003).

Figure S1 shows the experimental and predicted data obtained by the HPDM and SPM models for ammonium sorption by Ze-Na in single and binary system. It is showed that both HPDM and SPM models reproduced properly the experimental data by the particle control, indicating this mechanism as the rate-limiting step for ammonium uptake onto the zeolite.

3.4 Reusability of Ze-Na and Ze-K

Desorption with sodium hydroxide was carried out in order to regenerate the loaded zeolites and to recover ammonium as well as to obtain a concentrated ammonium effluent. After desorption step, pre-concentration factors (calculated as the ratio of the volumes of the solutions, before and after elution) between 5 and 35 were achieved, with a highest concentration of 0.5 g/L, which makes the concentrated effluent as a promising precursor for fertilizer production after concentration stage, i.e. using liquid-liquid membrane contactors (Sancho et al. 2017). Moreover, after the last sorption-desorption working cycle, loaded zeolites can be used as fertilizer after a separation process by filtration (Hermassi et al. 2017).

Treatments with hydroxides (e.g., NaOH, KOH) have been widely studied (M. Auerbach et al. 2003; Querol et al. 1996) as they activate the zeolite's surface by increasing the size of internal

porous and in consequence the specific surface. Regeneration can be described accordingly to Eqs. 3 and 4 for Ze-Na and Ze-K, respectively. The experimental data obtained after three consecutive sorption-regeneration cycles is summarized in Table Table 14. The data was also fitted to Langmuir and Freundlich isotherm models. The sorption capacity of both zeolites in single and binary system is shown in Figure 5.

$$\cong ZO\text{-}NH_4^+ + NaOH \leftrightarrow \cong ZO\text{-}Na^+ + NH_3 + H_2O \quad (1)$$

$$\cong ZO\text{-}NH_4^+ + KOH \leftrightarrow \cong ZO\text{-}K^+ + NH_3 + H_2O \quad (2)$$

Table 4. Equilibrium experiments results for three consecutive sorption regeneration cycles of ammonium onto Ze-Na (using NaOH 1 M) and Ze-K (using KOH 1 M).

		Ammonium single			Binary system		
		1st cycle	2nd cycle	3rd cycle	1st cycle	2nd cycle	3rd cycle
Ze-Na							
Langmuir	R^2	0.99	0.99	0.99	0.99	0.99	0.98
	K_L	$2.15x10^{-3}$	$4.57x10^{-3}$	$1.11x10^{-2}$	$2.17x10^{-2}$	$2.84x10^{-2}$	$1.36x10^{-2}$
	q_m	109±4	72±2	45±2	17±1	33±1	31±2
Freundlich	R^2	0.92	0.95	0.96	0.69	0.88	0.97
	K	1.65	1.43	2.12	1.20	1.85	3.14
	n	1.85	2.01	2.42	2.57	2.30	2.79
Ze-K							
Langmuir	R^2	0.99	0.99	0.99	0.99	0.98	0.99
	K_L	$1.14x10^{-2}$	$1.73x10^{-2}$	$1.33x10^{-2}$	$1.10x10^{-2}$	$1.34x10^{-2}$	$2.15x10^{-2}$
	q_m	21±2	40±2	41±2	29±1	43±2	37±1
Freun	R^2	0.88	0.90	0.95	0.91	0.93	0.94

	K	0.63	1.96	2.58	0.96	3.81	2.36
	n	1.86	2.29	2.66	2.02	2.94	2.57

In single system, ammonium loading capacity decreased after each sorption-desorption cycle, probably due to an incomplete desorption of ammonium which results in less available sites on the zeolite surface after each cycle (81% and 86% of desorption efficiency for first and second cycle, respectively). Moreover, adsorption constant (K) is increased cycle-by-cycle leading to more favored sorption conditions due to the alkaline activation of functional sites of zeolite (Otal et al. 2013; Wu et al. 2007; B.-H. Zhang et al. 2007).

Figure 5.

Ammonium sorption on Ze-Na in binary systems increased the loading capacity in the second working cycle as the loaded ammonium was fully extracted (99% of desorption efficiency) and the process of desorption activated functional sites on zeolite surface. A slightly decrease in the third working cycle was observed as the alkaline desorption not extracted all the sorbed ammonium after the second sorption-desorption working cycle (78% of desorption efficiency).

This behavior was also observed by Alshameri et al. (2014) who tested salt activated Chinese natural zeolites reporting a decrease of 45% in sorption capacity after 5 sorption-desorption working cycles. As discussed by W. Zhang et al. (2017), this could be explained as NH_4^+ adsorption into Ze-Na is carried out in two stages, surface adsorption and intra-particle diffusion. As alkaline regeneration desorbed almost all loaded ammonium by modifying porous and textural structure of zeolite, after regeneration, the ammonium uptake can be only performed by surface adsorption.

In the case of Ze-K, in both single and binary system, it was observed a loading capacity increase after the first sorption-desorption working cycle followed by a capacity stabilization. This fact could be explained by the zeolite surface alkaline activation by the elution solution and the achievement of high desorption efficiency (up to 90% in all cases).

Thus, despite Ze-K reported lower sorption capacity than Ze-Na in the first working cycle, it showed better performance after three sorption-desorption working cycles as sorbed ammonium can be recovered more efficiently and regenerated zeolite can be reused for subsequent sorption cycles. Then, although the cost of KOH is higher than NaOH, the excess of strong base used to regenerate the zeolite (NaOH/KOH) could be recovered and recycled to the zeolite regeneration stage under the scenario of post-treatment step.

Ammonium sorption mechanism onto both Ze-Na and Ze-K is mainly due to the ion exchange between ammonium ions present in aqueous solution and sodium and potassium ions present on the surface of zeolite as counter ion. As both EDS and XRD analysis shown the presence of calcium in the zeolite structure, calcium ions could contribute also to the ammonium uptake.

4. Conclusions

Modification of Ze-Na zeolite to its potassium form improved the sorbent regenerability and its capability to be desorbed and reused despite the lower initial ammonium sorption capacity. In single system the sorption capacity after the first cycle of Ze-Na and Ze-K were 109±4 mgNH_4/g and 21±3 mgNH_4/g, respectively; while in the third sorption cycle, the sorption capacity of both zeolites was around 45±6 mg NH_4/g. Then, Ze-K can be reused for several sorption-desorption cycles with no reduction but increase of maximum ammonium sorption capacity.

During the zeolite modification, sodium ions were fully exchanged by potassium ions at room temperature, as zeolites are more selective to potassium ions than sodium ions, thus the ion

306 exchange process is favoured. This selectivity also explains the reduction of ammonium sorption
307 capacity by Ze-K compared to the Ze-Na.

308 Neither Ze-Na nor Ze-K reported significant phosphate sorption capacity during the binary test,
309 indicating that a mixture of Ze-Na/Ze-K with sorbents capable to uptake phosphate from aqueous
310 solution such as zeolites in calcium, magnesium, aluminium or ferrous forms is necessary.

311 The reusability of Ze-Na and Ze-K as well as their low sorption capacity for phosphate ions
312 indicate that both sorbents can be reused and useful to obtain concentrated ammonium streams
313 but not for the use of the loaded zeolites as slow-release fertilizer since they do not contain
314 phosphate.

315 **5. Acknowledgment**

316 This study has been supported by the Waste2Product project (CTM2014-57302-R) financed by
317 Ministry of Science and Innovation and the Catalan government (project ref. 2014SGR050).
318 Authors also want to thank X. Querol and O. Font for providing the raw material as well as D. Qiu
319 for her dedication in experimental work.

320

321 **References**

322 Abdi, G. H., Khui, M. K., & Eshghi, S. (2006). Effects on natural zeolite on growth and flowering
323 on strawberry. *International Journal of Agricultural Research*, *1*, 384–389.

324 Alshameri, A., Yan, C., Al-Ani, Y., Dawood, A. S., Ibrahim, A., Zhou, C., & Wang, H. (2014). An
325 investigation into the adsorption removal of ammonium by salt activated Chinese (Hulaodu)
326 natural zeolite: Kinetics, isotherms, and thermodynamics. *Journal of the Taiwan Institute of*
327 *Chemical Engineers*, *45*(2), 554–564. doi:10.1016/j.jtice.2013.05.008

328 Auerbach, M., Carrado, K. a., & Dutta, P. K. (2003). *Handbook of Zeolite Science and*

329 *Technology*. *Science*.

330 Bassin, J. P., Kleerebezem, R., Dezotti, M., & van Loosdrecht, M. C. M. (2012). Simultaneous
331 nitrogen and phosphate removal in aerobic granular sludge reactors operated at different
332 temperatures. *Water research*, *46*(12), 3805–16. doi:10.1016/j.watres.2012.04.015

333 Diamantis, V., Eftaxias, A., Bundervoet, B., & Vestraete, W. (2014). Performance of the
334 biosorptive activated sludge (BAS) as pre-treatment to UF for decentralized wastewater
335 reuse. *Bioresource technology*, *156*, 314–321.

336 Ferrier, R. J., Cai, L., Lin, Q., Gorman, G. J., & Neethling, S. J. (2016). Models for apparent
337 reaction kinetics in heap leaching: A new semi-empirical approach and its comparison to
338 shrinking core and other particle-scale models. *Hydrometallurgy*, *166*, 22–33.

339 Gruener, J. E., Ming, D. W., Henderson, K. E., & Galindo, C. (2003). Common ion effects in
340 zeoponic substrates: Wheat plant growth experiment. *Microporous and Mesoporous*
341 *Materials*, *61*, 223–230.

342 Guaya, D., Valderrama, C., Farran, A., Armijos, C., & Cortina, J. L. (2015). Simultaneous
343 phosphate and ammonium removal from aqueous solution by a hydrated aluminum oxide
344 modified natural zeolite. *Chemical Engineering Journal*, *271*, 204–213.
345 doi:http://dx.doi.org/10.1016/j.ce.2015.03.003

346 Gupta, V., Sadegh, H., Yari, M., Shahryari Ghoshekandi, R., Maazinejad, B., & Chhardori, M.
347 (2015). Removal of ammonium ions from wastewater: A short review in development of
348 efficient methods. *Gobal Journal of Environmental Science and Management*, *1*(2), 71–94.

349 He, Y., Lin, H., Dong, Y., Liu, Q., & Wang, L. (2016). Simultaneous removal of ammonium and
350 phosphate by alkaline- activated and lanthanum-impregnated zeolite. *Chemosphere*, *164*,
351 387–395.

352 Hermassi, M., Valderrama, C., Gibert, O., Moreno, N., Querol, X., Batis, N. H., & Cortina, J. L.
353 (2017). Recovery of nutrients (N-P-K) from potassium-rich sludge anaerobic digestion side-
354 streams by integration of a hybrid sorption-membrane ultrafiltration process: Use of powder
355 reactive sorbents as nutrient carriers. *Science of the Total Environment*, *599–600*, 422–430.

356 Hua, Q. X., Zhou, J. M., Wang, H. Y., Du, C. W., Chen, X. Q., & Li, J. Y. (2006). Effects of
357 modified clinoptilolite on phosphorus mobilisation and potassium or ammonium release in
358 Ferrosols. *Australian Journal of Soil Research*, *44*, 285–290.

359 Huang, H., Yang, L., Xue, Q., Liu, J., Hou, L., & Ding, L. (2015). Removal of ammonium from
360 swine wastewater by zeolite combined with chlorination for regeneration. *Journal of*
361 *Environmental Management*, *160*, 333–341.
362 doi:http://dx.doi.org/10.1016/j.jenvman.2015.06.039

363 Jimenez, J., Miller, M., Bott, C., Murthy, S., De Clippeleir, H., & Wett, B. (2015). High-rate
364 activated sludge system for carbon management—evaluation of crucial process
365 mechanisms and design parameters. *Water Research*, *87*, 476–482.

366 Kim, Y.-S., Lee, Y.-H., An, B., Choi, S.-A., Park, J.-H., Jurng, J.-S., et al. (2012). Simultaneous
367 Removal of Phosphate and Nitrate in Wastewater Using High-Capacity Anion-Exchange
368 Resin. *Water, Air, & Soil Pollution*, *223*(9), 5959–5966. doi:10.1007/s11270-012-1331-1

369 Li, J., Qiu, J., Sun, Y., & Long, Y. (2000). Studies on natural STI zeolite: modification, structure,
370 adsorption and catalysis. *Microporous and Mesoporous Materials*, *37*, 365–378.

371 Lin, L., Lei, Z., Wang, L., Liu, X., Zhang, Y., Wan, C., et al. (2013). Adsorption mechanisms of
372 high-levels of ammonium onto natural and NaCl-modified zeolites. *Separation and*
373 *Purification Technology*, *103*, 15–20. doi:10.1016/j.seppur.2012.10.005

374 Marcelino, M., Wallaert, D., Guisasola, A., & Baeza, J. a. (2011). A two-sludge system for

simultaneous biological C, N and P removal via the nitrite pathway. *Water Science & Technology*, *64*(5), 1142. doi:10.2166/wst.2011.398

Mazloomi, F., & Jalali, M. (2016). Ammonium removal from aqueous solutions by natural Iranian zeolite in the presence of organic acids , cations and anions. *Journal of Environmental Chemical Engineering*, *4*, 1664–1673.

McGilloway, R., Weaver, R., Ming, D., & Gruener, J. E. (2003). Nitrification in a zeoponic substrate. *Plant Soil*, *256*, 371–378.

Mezohegyi, G., Bilad, M. R., & Vankelecom, I. F. J. (2012). Direct sewage up-concentration by submerged aerated and vibrated membranes. *Bioresource technology*, *118*, 1–7.

Millar, G. J., Winnett, A., Thompson, T., & Couperthwaite, S. J. (2016). Equilibrium studies of ammonium exchange with Australian natural zeolites. *Journal of Water Process Engineering*, *9*, 47–57.

Moreno, N., Querol, X., Ayora, C., Pereira, C. F., & Janssen-Jurkovicová, M. (2001). Utilization of zeolites synthesized from coal fly ash for the purification of acid mine waters. *Environmental Science and Technology*, *35*(17), 3526–3534. doi:10.1021/es0002924

Otal, E., Vilches, L. F., Luna, Y., Poblete, R., García-Maya, J. M., & Fernández-Pereira, C. (2013). Ammonium ion adsorption and settleability improvement achieved in a synthetic zeolite-amended activated sludge. *Chinese Journal of Chemical Engineering*, *21*(9), 1062–1068. doi:10.1016/S1004-9541(13)60566-2

Pauling, L. (1960). *The Nature of the Chemical Bond*. Ithaca: Cornell University Press. doi:978-0-8014-0333-0

Querol, X., Moreno, N., Alastuey, a, Juan, R., Ayora, C., Medinaceli, a, et al. (1996). Synthesis of high ion exchange zeolites from coal fly ash. *Geologica Acta*, *1*, 49–57.

Ramesh, K., Biswas, A. K., Somasundaram, J., & Subba Rao, A. (2010). Nanoporous zeolites in farming: Current status and issues ahead. *Current Science*, *99*(6), 760–765.

Ramesh, K., Reddy, D. D., Biswas, A. K., & Rao, A. S. (2011). Zeolites and Their Potential Uses in Agriculture. *Advances in Agronomy*, *113*, 215–236. doi:10.1016/B978-0-12-386473-4.00009-9

Sancho, I., Licon, E., Valderrama, C., de Arespacochaga, N., López-Palau, S., & Cortina, J. L. (2017). Recovery of ammonia from domestic wastewater effluents as liquid fertilizers by integration of natural zeolites and hollow fibre membrane contactors. *Science of The Total Environment*, *584–585*, 244–251.

Scherson, Y. D., & Criddle, C. S. (2014). Recovery of freshwater from wastewater: upgrading process configurations to maximize energy recovery and minimize residuals. *Environmental Science and Technology*, *48*(15), 8420–8432.

Sherry, H. S. (2003a). Ion Exchange. In S. M. Auerbach, K. A. Carrado, & P. K. Dutta (Eds.), *Handbook of Zeolite Science and Technology* (pp. 1006–1061). New York: Marcel Dekker, Inc.

Sherry, H. S. (2003b). Ion Exchange. In S. M. Auerbach, K. A. Carrado, & P. K. Dutta (Eds.), *Handbook of Zeolite Science and Technology* (pp. 1006–1061). New York: Marcel Dekker, Inc.

Takaya, C. A., Fletcher, L. A., Singh, S., Anyikude, K. U., & Ross, A. B. (2016). Phosphate and ammonium sorption capacity of biochar and hydrochar from different wastes. *Chemosphere*, *145*, 518–527. doi:10.1016/j.chemosphere.2015.11.052

Tashauoei, H. R., Movahedian, H. A., Amin, M. M., Kamali, M., Nikaeen, M., & Dastjerdi, V. M. (2010). Removal of cadmium and humic acid from aqueous solutions using surface modified

421 nanozeolite A. *International Journal of Environmental Science and Technology*, *7*(3), 497–
422 508.

423 Valderrama, C., Barios, J. I., Farran, A., & Cortina, J. L. (2010). Evaluation of Phenol/Aniline
424 (Single and Binary) Removal from Aqueous Solutions onto Hyper-cross-linked Polymeric
425 Resin (Macronet MN200) and Granular Activated Carbon in Fixed-Bed Column. *Water, Air,*
426 *& Soil Pollution*, *215*(1–4), 285–297. doi:10.1007/s11270-010-0478-x

427 Verstraete, W., & Vlaeminck, S. E. (2011). ZeroWasteWater: short-cycling of wastewater
428 resources for sustainable cities of the future. *Int. J. Sustainable Dev. World*, *18*(3), 253–264.

429 Wu, D., Hu, Z., Wang, X., He, S., & Kong, H. (2007). Use of zeolitized coal fly ash in the
430 simultaneous removal of ammonium and phosphate from aqueous solution. *Frontiers of*
431 *Environmental Science and Engineering in China*, *1*(2), 213–220. doi:10.1007/s11783-007-
432 0037-x

433 Wu, D., Zhang, B., Li, C., Zhang, Z., & Kong, H. (2006). Simultaneous removal of ammonium and
434 phosphate by zeolite synthesized from fly ash as influenced by salt treatment. *Journal of*
435 *colloid and interface science*, *304*(2), 300–6. doi:10.1016/j.jcis.2006.09.011

436 Yang, K., Zhang, X., Chao, C., Zhang, B., & Liu, J. (2014). In-situ preparation of NaA
437 zeolite/chitosan porous hybrid beads for removal of ammonium from aqueous solution.
438 *Carbohydrate Polymers*, *107*(1), 103–109. doi:10.1016/j.carbpol.2014.02.001

439 Yang, Y., Chen, Z., Wang, X., Zheng, L., & Gu, X. (2017). Partial nitrification performance and
440 mechanism of zeolite biological aerated filter for ammonium wastewater treatment.
441 *Bioresource Technology*, *241*, 473–481.

442 You, X., Farran, A., Guaya, D., Valderrama, C., Soldatov, V., & Cortina, J. L. (2016). Phosphate
443 removal from aqueous solutions using a hybrid fibrous exchanger containing hydrated ferric

444 oxide nanoparticles. *Journal of Environmental Chemical Engineering*, *4*, 388–397.

445 You, X., Guaya, D., Farran, A., Valderrama, C., & Cortina, J. L. (2015). Phosphate removal from
446 aqueous solution using a hybrid impregnated polymeric sorbent containing hydrated ferric
447 oxide (HFO). *Journal of Chemical Technology & Biotechnology*. doi:10.1002/jctb.4629

448 Zhang, B.-H., Wu, D.-Y., Wang, C., He, S.-B., Zhang, Z.-J., & Kong, H.-N. (2007). Simultaneous
449 removal of ammonium and phosphate by zeolite synthesized from coal fly ash as influenced
450 by acid treatment. *Journal of environmental sciences (China)*, *19*(5), 540–545.

451 Zhang, M., Zhang, H., Xu, D., Han, L., Niu, D., Tian, B., et al. (2011). Removal of ammonium from
452 aqueous solutions using zeolite synthesized from fly ash by a fusion method. *Desalination*,
453 *271*, 111–121.

454 Zhang, M., Zhang, H., Xu, D., Han, L., Niu, D., Zhang, L., et al. (2011). Ammonium removal from
455 aqueous solution by zeolites synthesized from low-calcium and high-calcium fly ashes.
456 *Desalination*, *277*(1–3), 46–53. doi:10.1016/j.desal.2011.03.085

457 Zhang, W., Zhou, Z., An, Y., Du, S., Ruan, D., Zhao, C., et al. (2017). Optimization for zeolite
458 regeneration and nitrogen removal performance of a hypochlorite-chloride regenerant.
459 *Chemosphere*, *178*, 565–572.

460 Zhang, X., Dong, L., Liang, Y., He, Y., Zhang, Y., & Zhang, J. (2013). Autotrophic nitrogen
461 removal from domestic sewage in MBR-CANON system and the biodiversity of functional
462 microbes. *Bioresource technology*, *150*, 113–120.

463

464

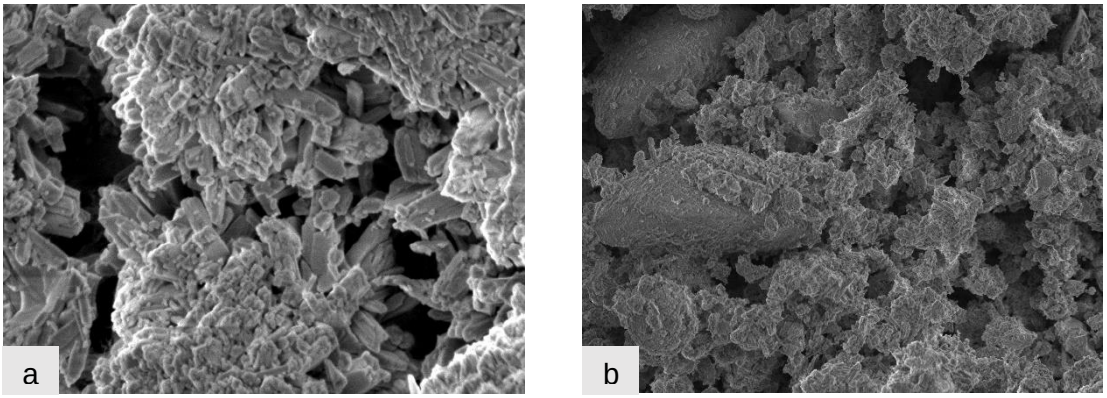

Figure 1. Scanning Electronic Microscopy of a) Ze-Na and b) Ze-K

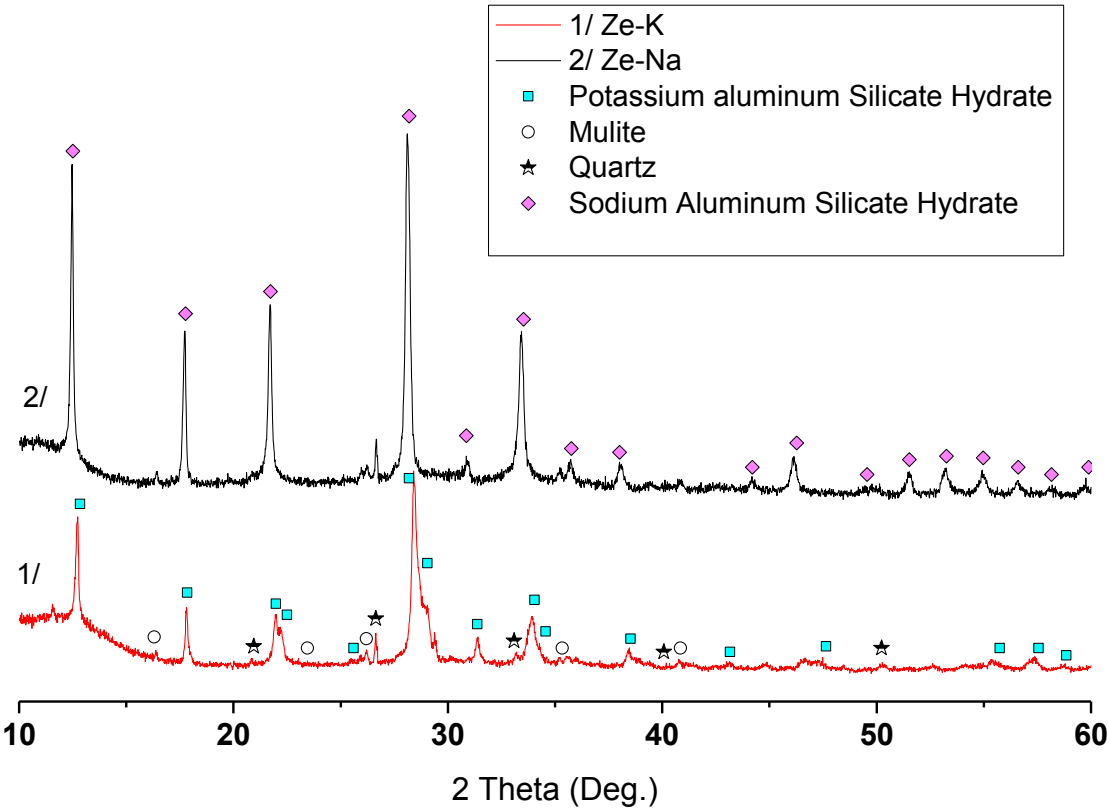

Figure 2. XRD pattern for Ze-Na and Ze-K.

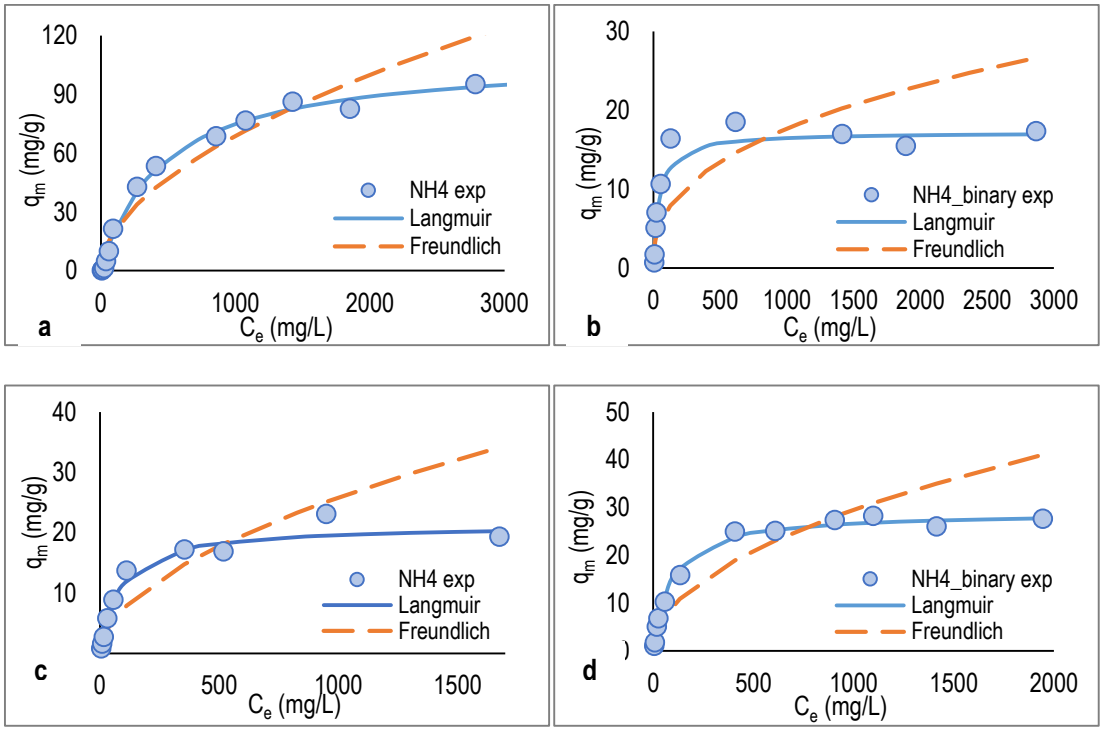

Figure 3. Experimental and theoretical equilibrium isotherm for ammonium removal by Ze-Na in a) single and b) binary system and by Ze-K in c) single and d) binary system.

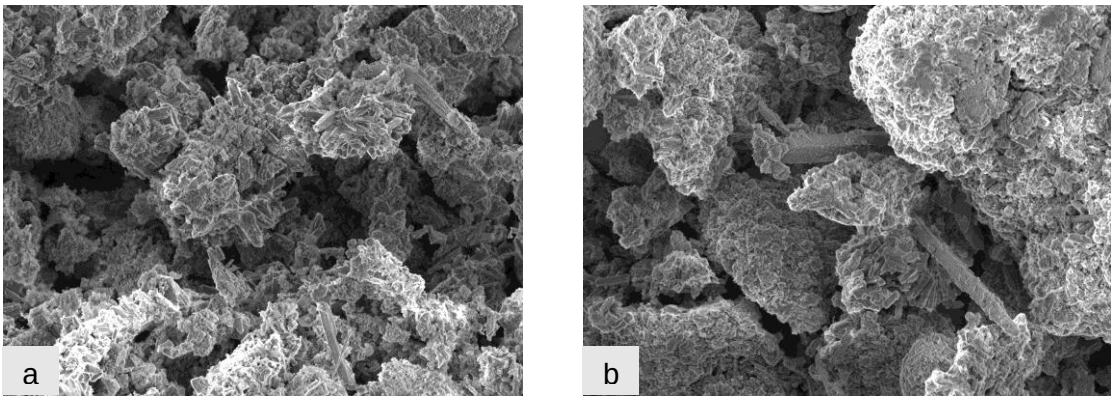

Figure 4. Scanning Electronic Microscopy of loaded a) Ze-Na and b) Ze-K

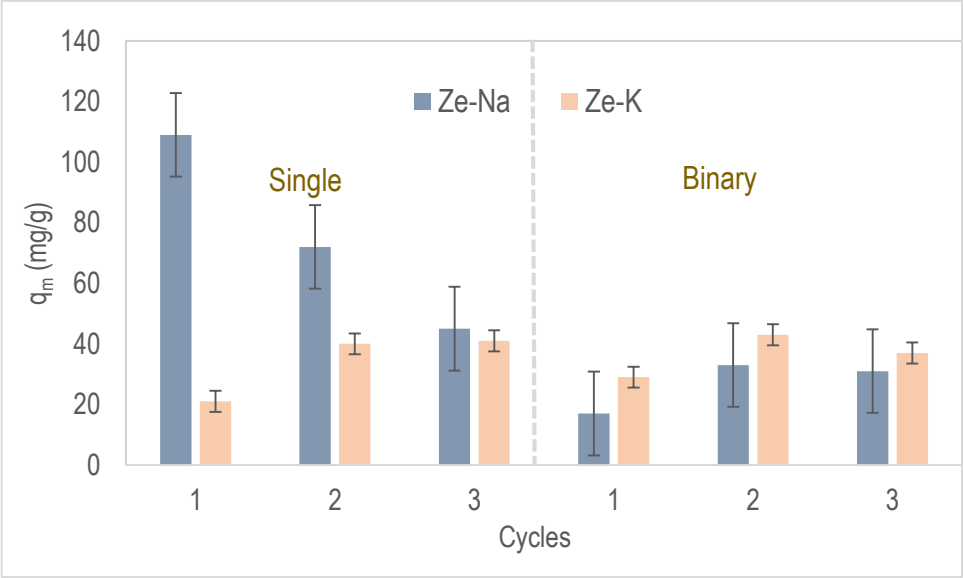

Figure 5. Sorption capacity evolution through three consecutive sorption-desorption cycles for Ze-Na and Ze-K in single and binary system.

Recovery of ammonium by powder synthetic zeolites from wastewater effluents: optimization of the regeneration step

Xialei You[a*], César Valderrama[a] , Xavier Querol[c] and José Luis Cortina[a,b]

[a] Department of Chemical Engineering. Universitat Politècnica de Catalunya-Barcelona-TECH (UPC), Spain

[b] Water Technology Center, CETaqua, Carretera d'Esplugues 75, Cornellá de Llobregat, 08940 Spain

[c] Institute of Environmental Assessment and Water Research IDAEA, Consejo Superior de Investigaciones Científicas (CSIC) Barcelona

[*]Correspondence should be addressed to: César Valderrama

Departament of Chemical Engineering, Universitat Politècnica de Catalunya-Barcelona Tech

Avda. Diagonal, 647 (08028) Barcelona, Spain

Tel.: 93 401 66 45

Email: cesar.alberto.valderrama@upc.edu

Supplementary Material

S1. Homogeneous Particle Diffusion Model

In this kinetic model, the adsorption mechanism involves diffusion of pollutants from the aqueous solution into the adsorbent phase through different stages. The rate-limiting step of adsorption can be described by either film diffusion where ions are diffused through the liquid film surrounding the particle or particle diffusion mechanism where ions are diffused into the adsorbent beads (El-Naggar et al. 2012).

Nernst-Plank equation (Helfferich 1962), which included both concentration and electrical gradients of exchanging ions into the flux equation, was used for establishing the HPDM equations. With diffusion rate controlling in the adsorption taking into account a spherical adsorbent, can be set equations depending on if particle diffusion (Eq. S2) or liquid film diffusion (Eq. S3) controls the rate of adsorption in function of the fractional attainment of equilibrium at time t (Eq. S1).

$$X(t) = \frac{q_t}{q_e} \qquad \text{Eq. S1}$$

$$-\ln(1 - X^2(t)) = \frac{2\pi^2 D_e}{r^2} t \qquad \text{Eq. S2}$$

$$-\ln(1 - X(t)) = \frac{3DC}{rC_r} t \qquad \text{Eq. S3}$$

Where q_t and q_e are the sorbent capacity at time t and in equilibrium [$mg \cdot g^{-1}$], D_e the effective diffusion coefficient of sorbates in the adsorbent [$m^2 \cdot s^{-1}$], r the radius of the adsorbent particle [m], D diffusion coefficient in solution phase [$m^2 \cdot s^{-1}$], C total concentration of adsorbing species [$mol \cdot dm^{-3}$] and C_r total concentration of adsorbing species in the adsorbent [$mol \cdot dm^{-3}$].

S2 Shell Progressive Model

When the porosity of the polymer is small and thus practically impervious to the fluid reactant, the adsorption process may be explained by the “shell progressive” approach. The kinetic concept of a “Shell Progressive” mechanism can be described in terms of the concentration profile of a liquid reactant containing a solute advancing into a spherical bead of a partially saturated adsorbent

(Valderrama et al. 2010) In this model can be defined three cases and the relationship between adsorption time and degree of adsorption is given by the following equations (Schmuckler and Golstein 1977). When the fluid film controls:

$$X = \frac{3C_{A0}K_F}{a_s r C_{S0}} t \qquad \text{Eq. S4}$$

When the diffusion through the adsorption layer controls:

$$3 - 3(1 - X)^{2/3} - 2X = \frac{6D_e C_{A0}}{a_s r^2 C_{S0}} t \qquad \text{Eq. S5}$$

When the chemical reaction controls:

$$1 - (1 - X)^{1/3} = \frac{k_s C_{A0}}{r} t \qquad \text{Eq. S6}$$

Where X is the fractional attainment of equilibrium at time t (Eq. S1), C_{A0} and C_{S0} are the concentration of adsorbing species A in bulk solution and at bead's unreacted core [mol·dm^{-3}], K_F the mass transfer coefficient of species A through the liquid film [m·s^{-1}], a_s the stoichiometric coefficient, r the radius of the adsorbent particle [m], D_e the effective diffusion coefficient of sorbates in the adsorbent [m^2·s^{-1}] and k_s the reaction constant based on surface [m^2·s^{-1}].

Table S1. Linear regression analysis of HPDM and SPM models for ammonium uptake on Na-Ze in single and multicomponent system

			Single	Binary
HPDM	-ln (1 - X^2)	D_e	2.57 x 10^{-11}	3.58 x 10^{-11}
		R^2	0.91	0.99
	-ln (1 - X)	D	3.79 x 10^{-7}	5.13 x 10^{-7}
		R^2	0.90	0.98

SPM	X	K_F	1.09×10^{-7}	3.26×10^{-8}
		R^2	0.85	0.53
	$[3 - 3(1 - X)^{2/3} - 2X]$	D_e	2.15×10^{-11}	2.29×10^{-11}
		R^2	0.88	0.92
	$[1 - (1 - X)^{1/3}]$	K_s	7.10×10^{-9}	7.99×10^{-9}
		R^2	0.87	0.92

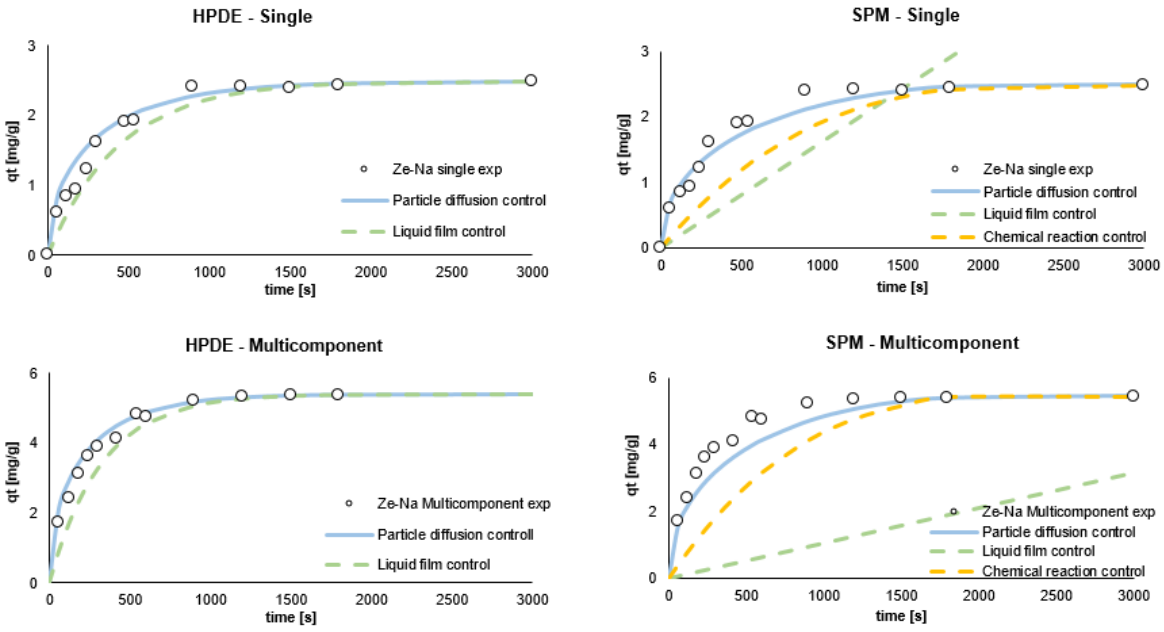

Figure S1. Ammonium sorption kinetics on Ze-Na and the theoretical curves obtained by the analysis of the HPDM and SPM models.

References:

I.M. El-Naggar, E.S. Zakaria, I.M. Ali, M. Khalil, M.F. El-Shahat, Kinetic modeling analysis for the removal of cesium ions from aqueous solutions using polyaniline titanotungstate, Arab. J. Chem. 5 (2012) 109–119.

F. Helfferich, Ion Exchange, Mc Graw Hill, New York, 1962.

C. Valderrama, J.I. Barios, M. Caetano, A. Farran, J.L. Cortina, Kinetic evaluation of phenol/aniline mixtures adsorption from aqueous solutions onto activated carbon and hypercrosslinked polymeric resin (MN200), React. Funct. Polym. 70 (2010) 142–150. doi:10.1016/j.reactfunctpolym.2009.11.003.

G. Schmuckler, S. Golstein, Chapter 1, in: J.A. Marisky, Y. Marcus (Eds.), Ion Exch. Solvent Extr. Vol. 7, Marcel Dekker, Inc., New York, 1977.